

Stress effects on excitons bound to shallow acceptors in GaAs

Martin Schmidt

Max-Planck-Institut für Festkörperforschung, 7 Stuttgart, Federal Republic of Germany

T. N. Morgan*

IBM Watson Research Center, Yorktown Heights, New York 10598

W. Schairer†

Max-Planck-Institut für Festkörperforschung, 7 Stuttgart, Federal Republic of Germany

(Received 18 February 1975)

We have performed stress-dependent photoluminescence measurements on excitons bound to neutral shallow acceptors (A^0X) in GaAs. From their temperature and stress variation three lines (at zero stress) are proved to be due to the decay of (A^0X) with the $J = 5/2$ state lowest. When low uniaxial stress ($0-2 \text{ kg mm}^{-2}$) is applied these three lines split into 7 or 8 components, although at high stress only one line remains with a stress shift equal to that for the conduction band to acceptor recombination. A theoretical interpretation based on a bonding two-hole state analogous to the H_2 molecule is found to agree well with the data when the effects of a weak crystal field are included. Small deviations between this theory and experiment are presumed to indicate the importance of the antibonding two-hole functions in the (A^0X) wave function.

I. INTRODUCTION

The edge photoluminescence spectra of epitaxial GaAs at helium temperature exhibit a complex of two or three sharp lines near 1.5122 eV. These lines have been found to be due to the recombination of excitons bound to shallow neutral acceptors (A^0X).¹ Using magnetic field emission spectra and optical absorption in comparison with line-strength calculations, White *et al.*² assigned the two main lines of the (A^0X) in InP and GaAs to the decay of the $J = \frac{5}{2}$ and $J = \frac{3}{2}$ states. The $J = \frac{5}{2}$ state was found to lie lower in energy, although the Zeeman spectra seemed to support the opposite assignment. A weak third line at higher energy was identified as the $J = \frac{1}{2}$ state.

Under uniaxial stress, the (A^0X) in InP was found to split into several well-resolved lines.³ Under the assumption of T_d symmetry and the absence of stress-induced interaction between the exciton states, Bailey⁴ calculated the stress splitting. In contrast, Morgan⁵ neglected both the crystal-field splitting of the two-hole state and the electron-hole exchange interaction in analysing the effect of uniaxial stress on the (A^0X) in GaSb.

We have performed photoluminescence measurements of the (A^0X) in GaAs under uniaxial stress to clarify the following questions: (i) What are the symmetries of the (A^0X) states? (ii) What is the influence of stress on the hole-hole and electron-hole interactions? (iii) Does the assignment of White *et al.* apply?

We shall show that the three lines belong to (A^0X) and can be labeled by the angular momentum quantum numbers $J = \frac{5}{2}$, $\frac{3}{2}$, and $\frac{1}{2}$ in order of in-

creasing energy, as identified in Ref. 2, although the former two states are mixed by a weak crystal field.

II. EXPERIMENTAL METHOD

The experimental arrangement is essentially the same as used in Ref. 6. In addition to the stress apparatus described there (range 2–70 kg, accuracy ~ 0.15 kg), an apparatus for low stress was used (range 0–10 kg, accuracy ~ 0.03 kg).

The undoped GaAs samples were grown by liquid-phase epitaxy and contained silicon and a little carbon as residual acceptors. By measuring samples with different levels of silicon and carbon we have determined that the amount of carbon in our samples was not nearly high enough to produce additional lines in the (A^0X) complex. The Hall carrier concentration of the n -type samples was $N_D - N_A = (3.1 \pm 0.2) \times 10^{15} \text{ cm}^{-3}$. The samples, typically $1.3 \times 1.3 \times 8 \text{ mm}$ were cut parallel to the three main lattice directions from a (110)-oriented wafer with an epitaxial surface. The stress was applied parallel to the long side of the slab.

III. EXPERIMENTAL RESULTS

A. Zero stress

At 4.2 K we observe three lines near 1.5122 eV, as shown in the inset in Fig. 1. The two strong lines are separated by 0.18 meV, and have half-widths of 0.06 meV. The weak line lies 0.42 meV higher than the lower line of the doublet and has a half-width of ~ 0.09 meV. In the following we shall label these lines by 5, 3, and 1 in order of increasing energy, according to the assignment J

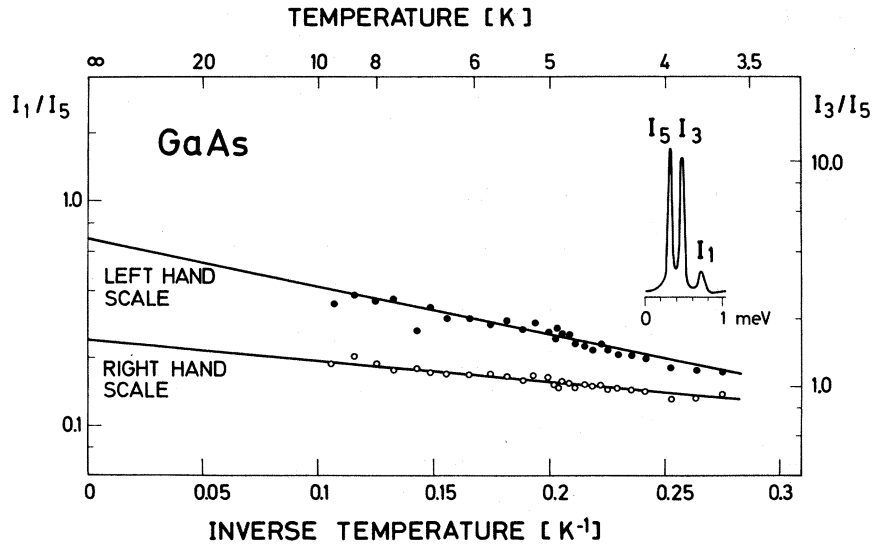


FIG. 1. Dependence of the relative line strengths I_1/I_5 and I_3/I_5 on temperature. The points are the experimental results; the lines are fits with a slope corresponding to the line spacing 0.42 meV for I_1/I_5 and 0.18 meV for I_3/I_5 . The spectrum is recorded at 4.2 K.

$= \frac{5}{2}$, $J = \frac{3}{2}$, and $J = \frac{1}{2}$ of White *et al.*²

To prove that all three lines belong to the same exciton complex we show in Fig. 1 the intensity ratios I_1/I_5 and I_3/I_5 in the temperature range 3.6–9.4 K. Two straight lines through the experimental points with slopes corresponding to -0.18 meV/ k for I_3/I_5 and -0.42 meV/ k for I_1/I_5 (k is Boltzmann's constant) show the thermal population of the higher states. The slopes have been taken from the energy separation of the lines.

The high-temperature intercepts of the straight lines in Fig. 1 give the ratios of the intrinsic line strengths, $I_1:I_3:I_5 = (0.7 \pm 0.2):(1.65 \pm 0.1):1$. The differences between these ratios and the theoretical ratios 1:4:1 calculated by White⁷ provide a measure of the effectiveness of the cubic crystal field in mixing the Γ_8 ($J = \frac{3}{2}$) state with the Γ_8 component of $J = \frac{5}{2}$. We discuss this mixing further in Sec. IV B.

B. High stress

Under low uniaxial stress the three (A^0X) lines split into seven resolvable components. When the stress is increased above 2 kg mm^{-2} only one line remains and shifts with [100], [111], or [110] stress in the same way as the band-acceptor recombination line. The half-width of this line is about 0.2 meV, increasing slightly with stress. It can be observed only up to $\sim 15 \text{ kg mm}^{-2}$, since at higher stress it overlaps the recombination line of the neutral donor bound exciton.

In the range 0–4 kg mm^{-2} the polarization ($I_\pi - I_\sigma)/(I_\pi + I_\sigma)$, where I_π and I_σ are the intensities parallel and perpendicular to the stress, respectively, increases from zero to nearly 60%. A 60% polarization is expected in the limit of high stress, where the transition is from $M_J = \pm \frac{1}{2}$ to

$M_J = \pm \frac{1}{2}$ (see below). However, in the range 4–15 kg mm^{-2} the polarization decreases linearly with different slopes in the three stress directions. Only a part of this stress dependence can be explained as due to the crystal field mixing. (See Sec. V, below.)

C. Low stress

The splitting of the three (A^0X) lines in the stress range 0–2 kg mm^{-2} is shown in Fig. 2 for stress parallel to the [100] direction. The splitting patterns using stress along the [111] and [110] directions are similar except that the slopes are different owing to different deformation potentials. The spectrometer polarization $I_\sigma/I_\pi = 2.2$ is not corrected in Fig. 2, since the much stronger π polarized spectra in the higher strain range would give a less clear picture. The details of Fig. 2 will be used in the discussion of the agreement of theory and experiment in Sec. V.

IV. THEORY

A. Without the crystal field

The complex (A^0X) consists of two holes and one electron weakly bound to a negative acceptor ion. The particles can be treated as effective mass particles with a spin of $\frac{1}{2}$ for the $s_{1/2}$ (Γ_6) electron and a quasispin of $\frac{3}{2}$ for each of the $p_{3/2}$ (Γ_8) holes. The binding resembles that of the two positive and two negative particles in the H_2 molecule except for the mass differences and spin differences which contribute to the exchange coupling of the two holes with each other and with the electron. In the following analysis we omit the complexities generated by the weak crystal field, mentioned above, until after we have developed the basic theory.

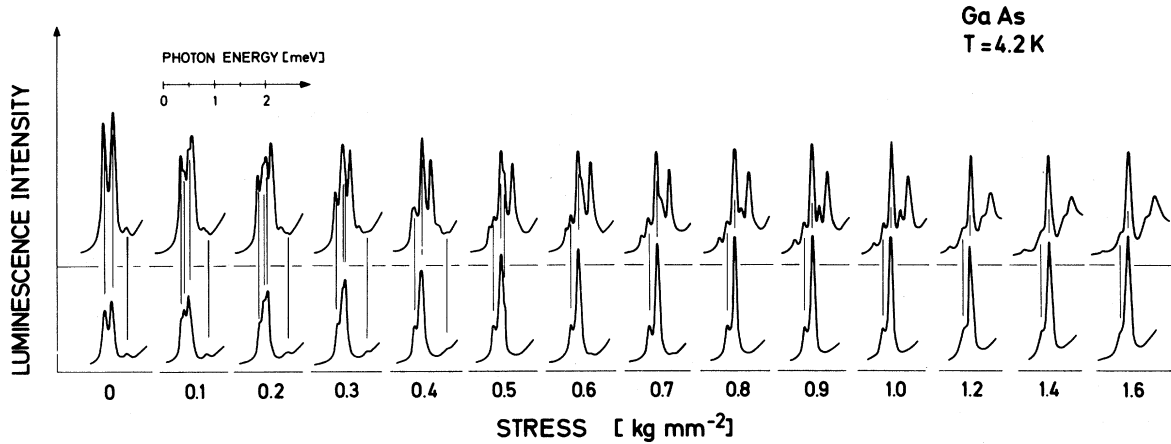


FIG. 2. Spectra of (A^0X) under increasing stress along the [100] direction for σ (upper spectra) and π (lower spectra) polarization.

By analogy with the H_2 molecule we assume that the ground state is composed primarily of the symmetric combination of the orbital or envelope functions of the two identical particles, the holes. Hence, by the exclusion principle the two-hole spin functions must be predominantly antisymmetric. The antisymmetric product of the two "spin" $-\frac{3}{2}$ hole wave functions contains an s -like singlet ($j=0$) and a d -like quintuplet ($j=2$) function, which couple to the spin- $\frac{1}{2}$ electron to form three states of angular momentum $J=\frac{1}{2}, \frac{3}{2},$ and $\frac{5}{2}$. See Fig. 3. The energetic ordering of the states, which can be deduced from the theory of atomic spectra,⁸ is as shown in Fig. 3 with $J=\frac{5}{2}$ lowest and $J=\frac{1}{2}$ highest. The forms of the wave functions can be written down by use of the angular momentum (Wigner) coupling coefficients.⁹ For the two holes, if we write the envelope functions as $g(r_i)$ and $h(r_i)$, $i=1, 2$, the $j=0$ and $j=2$ wave functions can be written $\psi_{j,m} = F(r_1, r_2) |j, m\rangle$, where $F = [g(r_1)h(r_2) + h(r_1)g(r_2)]/\sqrt{2}$, and the spin functions for $j=0, 2$ are

$$\begin{aligned}
 |0, 0\rangle &= \frac{1}{2}(|\frac{3}{2}\rangle_1 |-\frac{3}{2}\rangle_2 - |-\frac{3}{2}\rangle_1 |\frac{3}{2}\rangle_2 \\
 &\quad - |\frac{1}{2}\rangle_1 |-\frac{1}{2}\rangle_2 + |-\frac{1}{2}\rangle_1 |\frac{1}{2}\rangle_2), \\
 |2, \pm 2\rangle &= \pm(1/\sqrt{2})(|\pm\frac{3}{2}\rangle_1 |\pm\frac{3}{2}\rangle_2 - |\pm\frac{1}{2}\rangle_1 |\pm\frac{3}{2}\rangle_2), \\
 |2, \pm 1\rangle &= \pm(1/\sqrt{2})(|\pm\frac{3}{2}\rangle_1 |\mp\frac{1}{2}\rangle_2 - |\mp\frac{1}{2}\rangle_1 |\pm\frac{3}{2}\rangle_2), \\
 |2, 0\rangle &= \frac{1}{2}(|\frac{3}{2}\rangle_1 |-\frac{3}{2}\rangle_2 - |-\frac{3}{2}\rangle_1 |\frac{3}{2}\rangle_2 \\
 &\quad + |\frac{1}{2}\rangle_1 |-\frac{1}{2}\rangle_2 - |-\frac{1}{2}\rangle_1 |\frac{1}{2}\rangle_2),
 \end{aligned} \tag{2}$$

in terms of the basis "spin" functions $|m_s\rangle_i = |\frac{3}{2}, m_s\rangle$ of the i th hole for $s=\frac{3}{2}$. The exciton functions when written in terms of these and the electron spin functions $|\pm\frac{1}{2}\rangle_e$ are products of the three-particle envelope function $F(r_1, r_2)f(r_e)$ and the set of spin functions $|J, M_J\rangle$, where

$$\begin{aligned}
 |\frac{1}{2}, \pm\frac{1}{2}\rangle &= |0, 0\rangle |\pm\frac{1}{2}\rangle_e, \\
 |\frac{3}{2}, \pm\frac{3}{2}\rangle &= \pm(1/\sqrt{5})(2|2, \pm 2\rangle |\mp\frac{1}{2}\rangle_e - |2, \pm 1\rangle |\pm\frac{1}{2}\rangle_e), \\
 |\frac{3}{2}, \pm\frac{1}{2}\rangle &= \pm(1/\sqrt{5})(\sqrt{3}|2, \pm 1\rangle |\mp\frac{1}{2}\rangle_e - \sqrt{2}|2, 0\rangle |\pm\frac{1}{2}\rangle_e), \\
 |\frac{5}{2}, \pm\frac{5}{2}\rangle &= |2, \pm 2\rangle |\pm\frac{1}{2}\rangle_e, \\
 |\frac{5}{2}, \pm\frac{3}{2}\rangle &= (1/\sqrt{5})(|2, \pm 2\rangle |\mp\frac{1}{2}\rangle_e + 2|2, \pm 1\rangle |\pm\frac{1}{2}\rangle_e), \\
 |\frac{5}{2}, \pm\frac{1}{2}\rangle &= (1/\sqrt{5})(\sqrt{2}|2, \pm 1\rangle |\mp\frac{1}{2}\rangle_e + \sqrt{3}|2, 0\rangle |\pm\frac{1}{2}\rangle_e).
 \end{aligned} \tag{3}$$

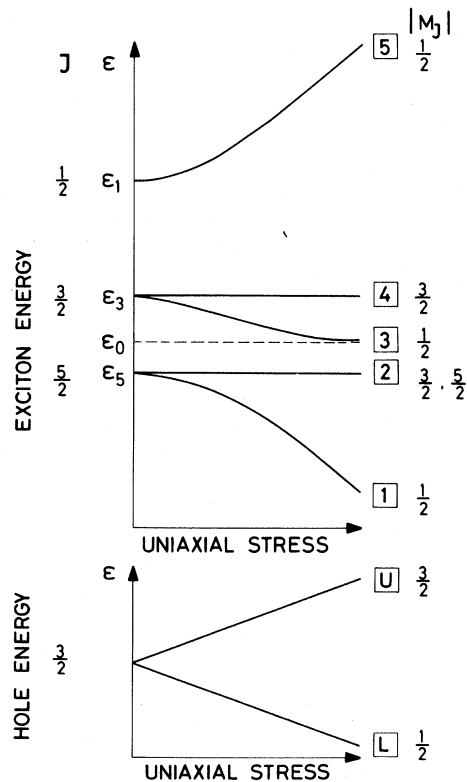


FIG. 3. Schematic plot of the splitting of the (A^0X) initial and ground states under uniaxial stress.

When uniaxial stress is applied to a crystal containing bound excitons described by these wave functions, the degeneracy of the states is lifted as a result of the splitting of the hole energies. From a knowledge of the strain splitting of the one-hole energy levels we can compute the two-hole shifts from Eqs. (2) and the exciton shifts from Eqs. (3). Because a small compressive uniaxial stress decreases the energy of the $m_s = \pm \frac{1}{2}$ hole levels (moving them toward the conduction band) by the same amount that the $m_s = \pm \frac{3}{2}$ are increased, the anti-symmetric two-hole levels described by the functions $|j, m\rangle$ of Eqs. (2) remain unshifted in energy.

The stress can, however, mix levels having different j values but the same azimuthal quantum number m . Hence, if we denote by $H_T = \pm E_T$ the shifts of the one-hole levels under stress, all matrix elements of the stress Hamiltonian in the set of states $|j, m\rangle$ of Eqs. (2) vanish except the two,

$$\langle 0, 0 | H_T | 2, 0 \rangle = \langle 2, 0 | H_T | 0, 0 \rangle = 2E_T. \quad (4)$$

Consequently, the two-hole eigenfunctions having $m \neq 0$ are unaltered by stress while those with $m = 0$ are mixed and approach, in the limit of large stress,

$$\psi_0^+ = (1/\sqrt{2})(|\frac{3}{2}\rangle_1 | -\frac{3}{2}\rangle_2 - | -\frac{3}{2}\rangle_1 |\frac{3}{2}\rangle_2), \quad (5)$$

at energy $2E_T$, and

$$\psi_0^- = (1/\sqrt{2})(|\frac{1}{2}\rangle_1 | -\frac{1}{2}\rangle_2 - | -\frac{1}{2}\rangle_1 |\frac{1}{2}\rangle_2),$$

at energy $-2E_T$.

The resulting energies of the levels are shown in Fig. 3. In the lower part of the figure is shown the stress-induced splitting of the final (one-hole) state after exciton decay and in the upper part the splitting and shifts of the initial states. The center-of-gravity shift due to the hydrostatic component of stress has been omitted from this figure. Note that the $|M_J| > \frac{1}{2}$ components are unshifted in this approximation and remain at the energies E_3 and E_5 of the unperturbed $J = \frac{3}{2}$ and $J = \frac{5}{2}$ states, respectively. The $M_J = \frac{1}{2}$ levels are coupled, however, as are the $M_J = -\frac{1}{2}$ ones, and form a set of three Kramers doublets whose energies E satisfy the cubic equation

$$(E_1 - E)(E_3 - E)(E_5 - E) = 4E_T^2 [C_-^2(E_3 - E) + C_+^2(E_5 - E)], \quad (6)$$

with $C_{\pm} = [(5 \pm 1)/10]^{1/2}$. At high stress the highest energy level (which begins at the unperturbed $J = \frac{1}{2}$ energy E_1) and the lowest level approach asymptotically the lines $E = \bar{E} \pm 2E_T$, while the middle level approaches the constant energy $E = E_0$. Here the two constants are

$$\bar{E} = \frac{1}{2}(E_1 + C_+^2 E_3 + C_-^2 E_5) = \frac{1}{10}(5E_1 + 2E_3 + 3E_5) \quad (7)$$

and

$$E_0 = C_-^2 E_3 + C_+^2 E_5 = \frac{1}{5}(3E_3 + 2E_5).$$

B. Crystal field

This would be the solution of the problem if no other interactions existed within the set of states, Eq. (3), which we are considering. However, as stated previously, the crystal field causes a significant mixing of the states from the $J = \frac{3}{2}$ and $\frac{5}{2}$ excitons which belong to the representation Γ_8 of the cubic group T_d of the crystal. In a subsequent publication we calculate the effect of this mixing on the wave functions and energies of the exciton states. We show there that the crystal field alters the results derived above in two important ways: (a) A Γ_7 Kramers doublet separates from the Γ_8 part of the $j = \frac{5}{2}$ state but retains only $\frac{1}{18}$ of the total emission intensity of the exciton. (b) The remaining Γ_8 part of the $J = \frac{5}{2}$ state mixes with the $J = \frac{3}{2}$ state. This redistributes the emission intensities of the lines, as noted above, and also alters the strain matrix elements. For [100] stress this mixing changes only the C_{\pm} of (6) and (7), but preserves the sum, $C_+^2 + C_-^2 = 1$.

V. COMPARISON WITH EXPERIMENT

The lines in Fig. 4 show the emission energies predicted (in the absence of a crystal field) for transitions between the initial- and final-state energy levels, with the center-of-gravity shift included. We have used the hydrostatic deformation potential $a' = -9.7$ eV and the [100] acceptor deformation potential $b' = -1.0$ eV.¹⁰ The labels identify the initial exciton energy levels (1-5) and the final upper (U) or lower (L) hole states.

The points in Fig. 4 have been taken from the data of Fig. 2. However, the measured stress values noted in Fig. 2 are somewhat in error because of the difficulty of eliminating friction in the stress apparatus at these small stresses. A more accurate stress calibration can be made directly from the measured splittings of the final hole states, i.e., the separation of a pair of lines derived from a single initial state. The raw data are sufficiently accurate to enable us to identify the two pairs of lines (1U, 1L) and (2U, 2L) over most of the stress range. (Note that line 1L, which is the only persistent line at high stress (see below), lies below its predicted value, near 3U.) Hence, an average of these two splittings has been used to refine the stress values—this required a shift of about 0.1 kg mm⁻² in the worst case—and the data have been plotted accordingly in Fig. 4.

The correction of these energy levels for the effect of the crystal field is easily made. The best fit with both the measured intensity ratios and the stress data is obtained for a crystal field strength and sign which shifts the Γ_7 level derived from

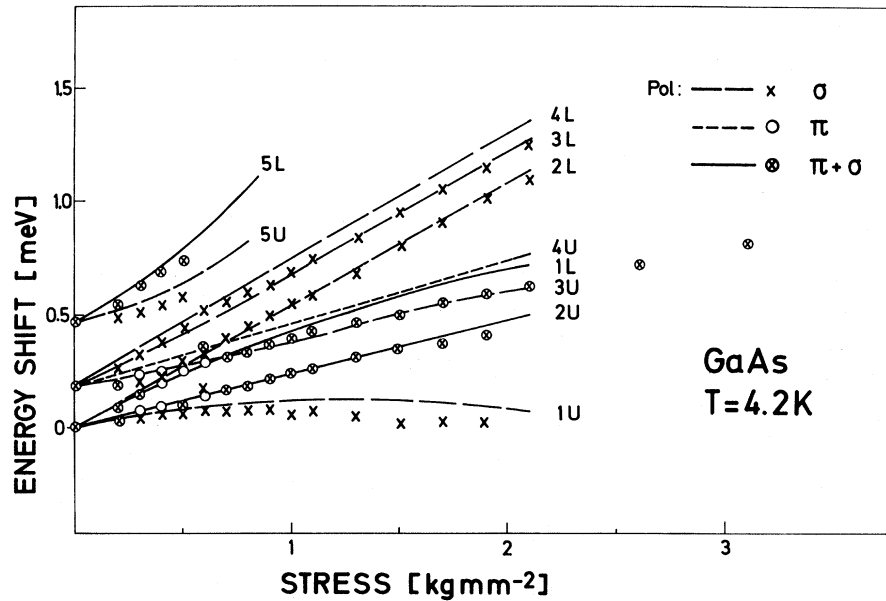


FIG. 4. Experimental (points) and calculated (lines) line shifts under increasing uniaxial stress. The stress is applied in a [100] direction.

$J = \frac{5}{2}$ to within about 0.01 meV of E_3 and changes C_+ in Eqs. (6) and (7) to $C_+ \approx 0$, $C_- = -1.00$. The fact that $C_+^2 \approx 0$ in Eq. (6) means that there should be no measurable stress splitting between energy levels 3 and 4 in Fig. 3 and that the entire stress dependence (other than the center of gravity shift) should appear in levels 1 and 5. We note further from Eq. (7) that since $\bar{E} = \frac{1}{2}(E_1 + E_5)$ is equal to E_3 within 0.03 meV, the emission lines 3U and 4U, at an energy of $E_3 - E_T$, should both approximately coincide with line 1L, at an energy of $\bar{E} - E_T$, for large stress.

With this one correction (moving lines 3U and 3L up to coincide with 4U and 4L, respectively) we can compare theory and experiment in Fig. 4. We find that only level 2 agrees with theory within experimental uncertainty over the entire range, while levels, 1, 3+4, and 5 lie significantly below their theoretical values. Level 4 can be uniquely identified only in the low-stress region, where 4U generates the parallel components derived from E_3 . It lies below its predicted value and is unresolvable from level 3 throughout the rest of the range, as expected.

The above discrepancies, as well as the stress dependence of the polarization mentioned above are presumed to be due to the admixture of some antibonding ($j=1, 3$) two-hole wave functions into the bonding ($j=1, 2$) ground states by the electron-hole exchange interaction. The lowering in energy of all levels (except one) below their predicted values is consistent with the appearance of a stress-dependent interaction with such higher-lying states. This will be discussed in a later publication. In the present work we note only that

agreement between theory and experiment is very good and allows us to isolate these higher order corrections.

The fact that only 1L persists to high stress is easily understood in terms of the thermalization of the initial exciton into its lowest $|M_J| = \frac{1}{2}$ level and the high-stress limit of this state. Since, at high stress, this lowest level is composed of almost purely $|m_s| = \frac{1}{2}$ holes, as Eq. (5) shows, transition 1U (into a $\frac{3}{2}$ hole level) vanishes and line 1L retains all of the oscillator strength.

VI. SUMMARY

We have presented photoluminescence measurements on the shallow neutral acceptor bound excitons in GaAs under uniaxial stress. A theory based on stress-induced interaction of the (A^0X) levels explains the experimental results. In particular we have shown: (i) All three observed lines are due to the decay of the (A^0X). (ii) A theoretical model based on symmetric (bonding) envelope wave functions combined with spin-like hole and electron Bloch functions, when corrected for a weak crystal field interaction, gives good agreement with experiment. (iii) The effect of uniaxial stress on the (A^0X) is well explained by the stress-induced interaction of the $|M_J| = \frac{1}{2}$ levels. (iv) The assignment of the three (A^0X) lines to the recombination of $J = \frac{5}{2}$, $\frac{3}{2}$, and $\frac{1}{2}$ initial states (in order of increasing energy) has been confirmed.

ACKNOWLEDGMENT

We are very grateful to Dr. E. Bauser for growing the high-quality GaAs samples and to Pro-

fessor H. J. Queisser for numerous discussions and his continued encouragement. One of us (T.N.M.) would like to thank the Alexander von

Humboldt Foundation and the Max-Planck-Institut for making possible a profitable year's stay at the Institute.

*Guest at the Max-Planck-Institute, 1973-1974.

†Present address: AEG-Telefunken, 71 Heilbronn, BRD, Germany.

¹Jagdeep Shah, R. C. C. Leite, and R. E. Nahory, *Phys. Rev.* **184**, 811 (1969).

²A. M. White, P. J. Dean, and B. Day, *J. Phys. C* **7**, 1400 (1974).

³See, for example, A. M. White, P. J. Dean, L. L. Taylor, R. C. Clarke, D. J. Ashen, and J. B. Mullin, *J. Phys. C* **5**, 1727 (1972).

⁴P. T. Bailey, *Phys. Rev. B* **1**, 588 (1970).

⁵Reference 17 of the article by C. Benoit à la Guillaume and P. Lavallard, *Phys. Rev. B* **5**, 4900 (1972).

⁶W. Schairer and M. Schmidt, *Phys. Rev. B* **10**, 2501 (1974).

⁷A. M. White, *J. Phys. C* **6**, 1971 (1973).

⁸E. U. Condon and G. H. Shortley, *The Theory of Atomic Spectra* (Cambridge U.P., Cambridge, England, 1935). Note in this reference the $\frac{3}{2}, \frac{3}{2}$ configuration of Fig. 4¹¹ and the $\frac{3}{2}, \frac{3}{2}, \frac{1}{2}$ configuration of Fig. 5¹¹ (with $\chi \gg 1$). In the latter the order of the $\frac{5}{2}$ and $\frac{3}{2}$ levels must be inverted to account for the negative charge on the electron relative to the holes.

⁹V. Heine, *Group Theory* (Pergamon, New York, 1960).

¹⁰The only fitting parameter to the experimental values is a' , whereas b' , which agrees with a value determined from a' and the stress-shift of the band-acceptor recombination line, has been taken from the splitting of the final hole state.